FERMILAB-Conf-95/215-E
D0

Single Photon, Photon-Jet and Diphoton Production at D0

S. Abachi et al.
The D0 Collaboration

Fermi National Accelerator Laboratory
P.O. Box 500, Batavia, Illinois 60510

July 1995

Submitted to the *International Europhysics Conference on High Energy Physics (HEP95)*, Brussels, Belgium, July 27-August 2, 1995

Operated by Universities Research Association Inc. under Contract No. DE-AC02-76CHO3000 with the United States Department of Energy

Single Photon, Photon-jet and Diphoton Production at DØ

The DØ Collaboration[1]

(July 1995)

Results are described on the observation of isolated single photons by the DØ detector at the Fermilab $\overline{p}p$ collider. The inclusive cross section has been measured for photons in the central rapidity region ($|\eta| < 0.9$) above 10 GeV E_T. Studies of jets recoiling against the single photon permit the measurement of the fundamental hard scattering $\cos\theta^*$ distribution. An analysis of the η correlations between high-E_T photons and the leading jet probes the gluon x distribution. Diphoton production measurements are used both as a test of QCD processes and as a search for resonant structure, including bosonic Higgs production.

S. Abachi,[12] B. Abbott,[34] M. Abolins,[23] B.S. Acharya,[41] I. Adam,[10] D.L. Adams,[35] M. Adams,[15] S. Ahn,[12] H. Aihara,[20] J. Alitti,[37] G. Álvarez,[16] G.A. Alves,[8] E. Amidi,[27] N. Amos,[22] E.W. Anderson,[17] S.H. Aronson,[3] R. Astur,[39] R.E. Avery,[29] A. Baden,[21] V. Balamurali,[30] J. Balderston,[14] B. Baldin,[12] J. Bantly,[4] J.F. Bartlett,[12] K. Bazizi,[7] J. Bendich,[20] S.B. Beri,[32] I. Bertram,[35] V.A. Bezzubov,[33] P.C. Bhat,[12] V. Bhatnagar,[32] M. Bhattacharjee,[11] A. Bischoff,[7] N. Biswas,[30] G. Blazey,[12] S. Blessing,[13] P. Bloom,[5] A. Boehnlein,[12] N.I. Bojko,[33] F. Borcherding,[12] J. Borders,[36] C. Boswell,[7] A. Brandt,[12] R. Brock,[23] A. Bross,[12] D. Buchholz,[29] V.S. Burtovoi,[33] J.M. Butler,[12] D. Casey,[36] H. Castilla-Valdez,[9] D. Chakraborty,[39] S.-M. Chang,[27] S.V. Chekulaev,[33] L.-P. Chen,[20] W. Chen,[39] L. Chevalier,[37] S. Chopra,[32] B.C. Choudhary,[7] J.H. Christenson,[12] M. Chung,[15] D. Claes,[39] A.R. Clark,[20] W.G. Cobau,[21] J. Cochran,[7] W.E. Cooper,[12] C. Cretsinger,[36] D. Cullen-Vidal,[4] M.A.C. Cummings,[14] D. Cutts,[4] O.I. Dahl,[20] K. De,[42] M. Demarteau,[12] R. Demina,[27] K. Denisenko,[12] N. Denisenko,[12] D. Denisov,[12] S.P. Denisov,[33] W. Dharmaratna,[13] H.T. Diehl,[12] M. Diesburg,[12] G. Di Loreto,[23] R. Dixon,[12] P. Draper,[42] J. Drinkard,[6] Y. Ducros,[37] S.R. Dugad,[41] S. Durston-Johnson,[36] D. Edmunds,[23] J. Ellison,[7] V.D. Elvira,[12,‡] R. Engelmann,[39] S. Eno,[21] G. Eppley,[35] P. Ermolov,[24] O.V. Eroshin,[33] V.N. Evdokimov,[33] S. Fahey,[23] T. Fahland,[4] M. Fatyga,[3] M.K. Fatyga,[36] J. Featherly,[3] S. Feher,[39] D. Fein,[2] T. Ferbel,[36] G. Finocchiaro,[39] H.E. Fisk,[12] Yu. Fisyak,[24] E. Flattum,[23] G.E. Forden,[2] M. Fortner,[28] K.C. Frame,[23] P. Franzini,[10] S. Fuess,[12] A.N. Galjaev,[33] E. Gallas,[42] C.S. Gao,[12,*] S. Gao,[12,*] T.L. Geld,[23] R.J. Genik II,[23] K. Genser,[12] C.E. Gerber,[12,§] B. Gibbard,[3] V. Glebov,[36] S. Glenn,[5] B. Gobbi,[29] M. Goforth,[13] A. Goldschmidt,[20] B. Gómez,[1] P.I. Goncharov,[33] H. Gordon,[3] L.T. Goss,[43] N. Graf,[3] P.D. Grannis,[39] D.R. Green,[12] J. Green,[28] H. Greenlee,[12] G. Griffin,[6] N. Grossman,[12] P. Grudberg,[20] S. Grünendahl,[36] W. Gu,[12,*] G. Guglielmo,[31] J.A. Guida,[39] J.M. Guida,[3] W. Guryn,[3] S.N. Gurzhiev,[33] P. Gutierrez,[31] Y.E. Gutnikov,[33] N.J. Hadley,[21] H. Haggerty,[12] S. Hagopian,[13] V. Hagopian,[13] K.S. Hahn,[36] R.E. Hall,[6] S. Hansen,[12] R. Hatcher,[23] J.M. Hauptman,[17] D. Hedin,[28] A.P. Heinson,[7] U. Heintz,[12] R. Hernández-Montoya,[9] T. Heuring,[13] R. Hirosky,[13] J.D. Hobbs,[12] B. Hoeneisen,[1,¶] J.S. Hoftun,[4] F. Hsieh,[22] Ting Hu,[39] Tong Hu,[16] T. Huehn,[7] S. Igarashi,[12] A.S. Ito,[12] E. James,[2] J. Jaques,[30] S.A. Jerger,[23] J.Z.-Y. Jiang,[39] T. Joffe-Minor,[29] H. Johari,[27] K. Johns,[2] M. Johnson,[12] H. Johnstad,[40]

[1] Submitted to the XVII International Symposium on Lepton-Photon Interactions (LP95), Beijing, China, August 10-15, 1995.

A. Jonckheere,[12] M. Jones,[14] H. Jöstlein,[12] S.Y. Jun,[29] C.K. Jung,[39] S. Kahn,[3] G. Kalbfleisch,[31] J.S. Kang,[18] R. Kehoe,[30] M.L. Kelly,[30] A. Kernan,[7] L. Kerth,[20] C.L. Kim,[18] S.K. Kim,[38] A. Klatchko,[13] B. Klima,[12] B.I. Klochkov,[33] C. Klopfenstein,[39] V.I. Klyukhin,[33] V.I. Kochetkov,[33] J.M. Kohli,[32] D. Koltick,[34] A.V. Kostritskiy,[33] J. Kotcher,[3] J. Kourlas,[26] A.V. Kozelov,[33] E.A. Kozlovski,[33] M.R. Krishnaswamy,[41] S. Krzywdzinski,[12] S. Kunori,[21] S. Lami,[39] G. Landsberg,[12] R.E. Lanou,[4] J-F. Lebrat,[37] A. Leflat,[24] H. Li,[39] J. Li,[42] Y.K. Li,[29] Q.Z. Li-Demarteau,[12] J.G.R. Lima,[8] D. Lincoln,[22] S.L. Linn,[13] J. Linnemann,[23] R. Lipton,[12] Y.C. Liu,[29] F. Lobkowicz,[36] S.C. Loken,[20] S. Lökös,[39] L. Lueking,[12] A.L. Lyon,[21] A.K.A. Maciel,[8] R.J. Madaras,[20] R. Madden,[13] I.V. Mandrichenko,[33] Ph. Mangeot,[37] S. Mani,[5] B. Mansoulié,[37] H.S. Mao,[12,*] S. Margulies,[15] R. Markeloff,[28] L. Markosky,[2] T. Marshall,[16] M.I. Martin,[12] M. Marx,[39] B. May,[29] A.A. Mayorov,[33] R. McCarthy,[39] T. McKibben,[15] J. McKinley,[23] T. McMahon,[31] H.L. Melanson,[12] J.R.T. de Mello Neto,[8] K.W. Merritt,[12] H. Miettinen,[35] A. Milder,[2] A. Mincer,[26] J.M. de Miranda,[8] C.S. Mishra,[12] M. Mohammadi-Baarmand,[39] N. Mokhov,[12] N.K. Mondal,[41] H.E. Montgomery,[12] P. Mooney,[1] M. Mudan,[26] C. Murphy,[16] C.T. Murphy,[12] F. Nang,[4] M. Narain,[12] V.S. Narasimham,[41] A. Narayanan,[2] H.A. Neal,[22] J.P. Negret,[1] E. Neis,[22] P. Nemethy,[26] D. Nešić,[4] D. Norman,[43] L. Oesch,[22] V. Oguri,[8] E. Oltman,[20] N. Oshima,[12] D. Owen,[23] P. Padley,[35] M. Pang,[17] A. Para,[12] C.H. Park,[12] Y.M. Park,[19] R. Partridge,[4] N. Parua,[41] M. Paterno,[36] J. Perkins,[42] A. Peryshkin,[12] M. Peters,[14] H. Piekarz,[13] Y. Pischalnikov,[34] A. Pluquet,[37] V.M. Podstavkov,[33] B.G. Pope,[23] H.B. Prosper,[13] S. Protopopescu,[3] D. Pušeljić,[20] J. Qian,[22] P.Z. Quintas,[12] R. Raja,[12] S. Rajagopalan,[39] O. Ramirez,[15] M.V.S. Rao,[41] P.A. Rapidis,[12] L. Rasmussen,[39] A.L. Read,[12] S. Reucroft,[27] M. Rijssenbeek,[39] T. Rockwell,[23] N.A. Roe,[20] P. Rubinov,[39] R. Ruchti,[30] S. Rusin,[24] J. Rutherfoord,[2] A. Santoro,[8] L. Sawyer,[42] R.D. Schamberger,[39] H. Schellman,[29] J. Sculli,[26] E. Shabalina,[24] C. Shaffer,[13] H.C. Shankar,[41] R.K. Shivpuri,[11] M. Shupe,[2] J.B. Singh,[32] V. Sirotenko,[28] W. Smart,[12] A. Smith,[2] R.P. Smith,[12] R. Snihur,[29] G.R. Snow,[25] S. Snyder,[39] J. Solomon,[15] P.M. Sood,[32] M. Sosebee,[42] M. Souza,[8] A.L. Spadafora,[20] R.W. Stephens,[42] M.L. Stevenson,[20] D. Stewart,[22] D.A. Stoianova,[33] D. Stoker,[6] K. Streets,[26] M. Strovink,[20] A. Taketani,[12] P. Tamburello,[21] J. Tarazi,[6] M. Tartaglia,[12] T.L. Taylor,[29] J. Teiger,[37] J. Thompson,[21] T.G. Trippe,[20] P.M. Tuts,[10] N. Varelas,[23] E.W. Varnes,[20] P.R.G. Virador,[20] D. Vititoe,[2] A.A. Volkov,[33] A.P. Vorobiev,[33] H.D. Wahl,[13] G. Wang,[13] J. Wang,[12,*] L.Z. Wang,[12,*] J. Warchol,[30] M. Wayne,[30] H. Weerts,[23] F. Wen,[13] W.A. Wenzel,[20] A. White,[42] J.T. White,[43] J.A. Wightman,[17] J. Wilcox,[27] S. Willis,[28] S.J. Wimpenny,[7] J.V.D. Wirjawan,[43] J. Womersley,[12] E. Won,[36] D.R. Wood,[12] H. Xu,[4] R. Yamada,[12] P. Yamin,[3] C. Yanagisawa,[39] J. Yang,[26] T. Yasuda,[27] C. Yoshikawa,[14] S. Youssef,[13] J. Yu,[36] Y. Yu,[38] Y. Zhang,[12,*] Y.H. Zhou,[12,*] Q. Zhu,[26] Y.S. Zhu,[12,*] Z.H. Zhu,[36] D. Zieminska,[16] A. Zieminski,[16] and A. Zylberstejn[37]

[1]Universidad de los Andes, Bogotá, Colombia
[2]University of Arizona, Tucson, Arizona 85721
[3]Brookhaven National Laboratory, Upton, New York 11973
[4]Brown University, Providence, Rhode Island 02912
[5]University of California, Davis, California 95616
[6]University of California, Irvine, California 92717
[7]University of California, Riverside, California 92521
[8]LAFEX, Centro Brasileiro de Pesquisas Físicas, Rio de Janeiro, Brazil
[9]CINVESTAV, Mexico City, Mexico
[10]Columbia University, New York, New York 10027
[11]Delhi University, Delhi, India 110007
[12]Fermi National Accelerator Laboratory, Batavia, Illinois 60510
[13]Florida State University, Tallahassee, Florida 32306
[14]University of Hawaii, Honolulu, Hawaii 96822

[15]University of Illinois at Chicago, Chicago, Illinois 60607
[16]Indiana University, Bloomington, Indiana 47405
[17]Iowa State University, Ames, Iowa 50011
[18]Korea University, Seoul, Korea
[19]Kyungsung University, Pusan, Korea
[20]Lawrence Berkeley Laboratory and University of California, Berkeley, California 94720
[21]University of Maryland, College Park, Maryland 20742
[22]University of Michigan, Ann Arbor, Michigan 48109
[23]Michigan State University, East Lansing, Michigan 48824
[24]Moscow State University, Moscow, Russia
[25]University of Nebraska, Lincoln, Nebraska 68588
[26]New York University, New York, New York 10003
[27]Northeastern University, Boston, Massachusetts 02115
[28]Northern Illinois University, DeKalb, Illinois 60115
[29]Northwestern University, Evanston, Illinois 60208
[30]University of Notre Dame, Notre Dame, Indiana 46556
[31]University of Oklahoma, Norman, Oklahoma 73019
[32]University of Panjab, Chandigarh 16-00-14, India
[33]Institute for High Energy Physics, 142-284 Protvino, Russia
[34]Purdue University, West Lafayette, Indiana 47907
[35]Rice University, Houston, Texas 77251
[36]University of Rochester, Rochester, New York 14627
[37]CEA, DAPNIA/Service de Physique des Particules, CE-SACLAY, France
[38]Seoul National University, Seoul, Korea
[39]State University of New York, Stony Brook, New York 11794
[40]SSC Laboratory, Dallas, Texas 75237
[41]Tata Institute of Fundamental Research, Colaba, Bombay 400005, India
[42]University of Texas, Arlington, Texas 76019
[43]Texas A&M University, College Station, Texas 77843

INTRODUCTION

Direct photons have proved to be a valuable tool for studying QCD at hadron colliders (1). Photons are a direct link to the parton level of the interaction, without ambiguities in identification and energy measurement. At low E_T, the dominant mode of production is from gluon Compton scattering, which makes the outgoing photon a good probe of the incoming gluon. At Tevatron energies ($\sqrt{s} = 1.8$ TeV) the gluon distributions as low as $x_g = 0.001$ can be probed with the DØ detector (2).

TRIGGER AND EVENT SELECTION

DØ operates with a multi-tier triggering system. The first level consists of scintillator near the beam pipe used to detect a $\overline{p}p$ interaction. The next level is a hardware trigger which makes fast sums of the electromagnetic energy in the calorimeter towers ($\Delta\eta = \Delta\phi = 0.2$). There were three hardware triggers used in these analyses with minimum E_T thresholds of 2.5, 7, and 10 GeV. The final level is a software based trigger which clusters the calorimeter cells and rejects the candidate if the longitudinal energy deposition is inconsistent with that expected from studies of Monte Carlo simulated electrons. The three E_T thresholds used in the software trigger were 6, 14, and 30 GeV.

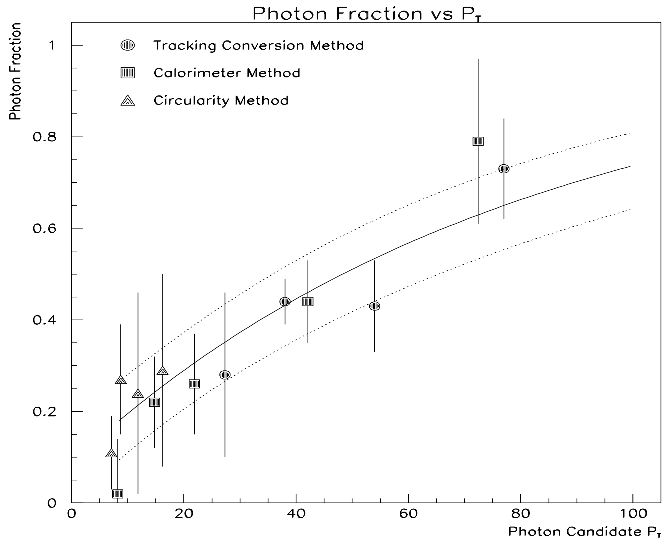

FIG. 1. Photon Fraction (γ) vs p_T^γ for the three methods of background subtraction. The solid line is a fit and the dotted lines are the errors of the fit.

Additional cuts are applied to the photon candidates offline. An $|\ \eta\ | < 0.9$ cut is used to restrict candidates to the central region. The electromagnetic fraction of the calorimeter shower must be greater than 96% of the total cluster energy, and the shower shape is required to be consistent with the shape of test beam electrons. An isolation cut of less than 2 GeV of E_T in the isolation cone $(0.2 < R < 0.4, R = \sqrt{\Delta\eta^2 + \Delta\phi^2}\ )$ is applied. The missing E_T ($\not\!\!E_T$) of the event is required to be less than 50% of the photon E_T (if the photon E_T is greater than 20 GeV) to reject electrons from W events.

BACKGROUND SUBTRACTION

The data sample detailed above contains a significant amount of background in the form of electromagnetic jets. These are mostly single isolated π^0's and η's which decay into two photons. In this p_T range ($p_{T\gamma} \geq 10$ GeV) the photons coalesce and mimic a single photon shower in the calorimeter. Fluctuations in the shower development make background subtraction on an event-by-event basis impossible. There are, however, methods by which the background can be subtracted on a statistical basis.

DØ uses three methods of background subtraction. They are all based on the relationship:

$$\gamma = \frac{\epsilon_\pi - \epsilon}{\epsilon_\pi - \epsilon_\gamma}. \tag{1}$$

where γ is the fraction of candidates that fulfill the selection criteria which are genuine direct photons, and ϵ_γ, ϵ_π, and ϵ are the fraction of candidates passing a specific cut for photons, background, and data respectively.

The first method uses the fact that the two-photon backgrounds tend to convert (produce e^+e^- pairs) roughly twice as often as single photons. This means that calorimeter showers from background develop earlier than single photon showers. The ratio of energy in the first layer of the calorimeter to the total shower energy is used as a discriminant.

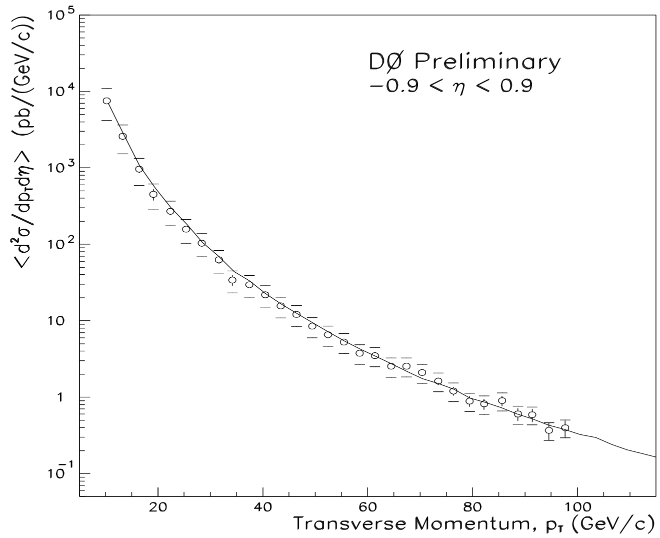

FIG. 2. The inclusive differential direct photon cross section as a function $p_{T\gamma}$. The theoretical prediction is NLO QCD (J. Owens) using CTEQ2M pdf's and $\mu = p_T$.

The second method is also based on backgrounds having a higher conversion probability. Conversions are tagged as tracks with twice minimum ionizing energy using the dE/dx measurement in the Central Drift Chambers.

The third method exploits the opening angle between the two photons from background sources. At lower p_T, this angle is large enough to create an asymmetry in the transverse shape of calorimeter showers. The shower profile becomes ellipsoidal rather than circular. We define a variable, circularity, as the ratio of the minor and major axes of the ellipse. For photons circularity should be close to unity (circular), whereas for π^0's and η's it tends to smaller values (asymmetric). This method is only used up to 20 GeV, above which the opening angle between the two photons is too small to be resolved in the calorimeter.

The photon fractions for the three background subtraction methods are shown in Fig. 1. A functional form of $\gamma(p_T)$ is obtained by fitting the three background subtraction methods and this function is used to subtract the background from the cross-section. The parameters in the fit are shifted by one standard deviation and the variation in $\gamma(p_T)$ is used as an estimate of the error.

INCLUSIVE PHOTON CROSS SECTION

The differential cross section as a function of p_T is shown in Fig. 2. The theory prediction is generated from a Monte Carlo generator based on next-to-leading order (NLO) QCD due to J. Owens with CTEQ2M parton distributions (3) and a renormalization scale of $\mu = p_T$. Figure 3 shows a plot of (DATA-THEORY)/THEORY to illustrate the good agreement between the two. In both figures, the inner error bars indicate the statistical error while the outer error bars indicate the systematic error. The shaded band at the bottom of the Fig. 3 corresponds to a $\pm 12\%$ normalization error due to the uncertainty in the luminosity.

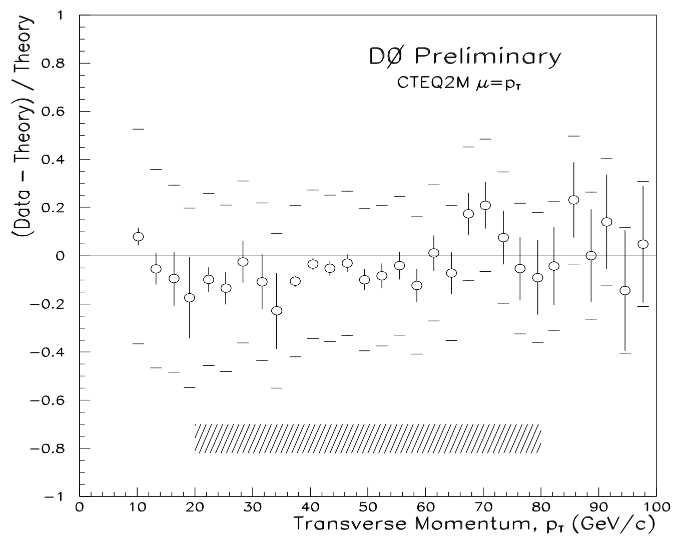

FIG. 3. Comparison between data and theory.

THE PHOTON ANGULAR DISTRIBUTION

Photon angular distributions may also prove to be a valuable tool for testing QCD. At the energies considered for this analysis, the dominant QCD jet processes occur via an interchange of a gluon (spin 1) propagator. This produces the characteristic angular distribution $dN/d\cos\theta^* \propto (1-\cos\theta^*)^{-2}$, where θ^* represents the photon-jet center of mass (CM) polar angle between the beam and the outgoing photon. Photons, on the other hand, are produced predominantly through processes involving the exchange of a spin 1/2 quark, which produces a distribution $dN/d\cos\theta^* \propto (1-\cos\theta^*)^{-1}$. This means that at relatively large $\cos\theta^* \geq 0.8$, the increase in the rate of production relative to $\cos\theta^* = 0$ is much larger for jets than for photons. This makes sensitive tests of QCD possible. Forward coverage is particularly important in this measurement.

For the preliminary analysis described here, all candidate photons with a p_T in excess of 30 GeV/c were recorded. In order to be able to reconstruct the kinematics of the event in the CM frame, it is also necessary to know the direction of the recoiling jets. Therefore, we require that at least one jet passing all standard jet quality cuts, was found in the event, and that $\not{E}_T \leq 0.3 p_{T\gamma}$. Furthermore, in order to retain the simplicity of the $2 \rightarrow 2$ process, we take the vector sum of all jets which are in the opposite hemisphere from the photon in ϕ. Additional cuts are placed on the azimuthal difference between the photon and the opposite summed jet ($|\phi_\gamma - \phi_j| < 0.3$) and the energy difference to ensure the $2 \rightarrow 2$ nature of the event. The measured quantities we extract from each event are η_γ, $E_{T\gamma}$, and η_{jet}. From these, we can form the CM quantities and the boost of that system relative to the lab,

$$\eta^* = \frac{\eta_\gamma - \eta_{jet}}{2}, \qquad \eta_{boost} = \frac{\eta_\gamma + \eta_{jet}}{2}, \qquad p^* = p_T \cdot \cosh\eta^*, \qquad \cos\theta^* = \tanh\eta^* \qquad (2)$$

Since we wish to cover as large a range in $\cos\theta^*$ (and therefore η^*) as possible, while requiring the photon to be central, we allow the recoil jet to cover a large range of pseudorapidity. In order to avoid acceptance corrections, we divide the data into three regions, each of which covers a range of 0.8 in η^* and η_{boost}. These regions form squares in η^* and η_{boost} space. The regions and their relationship to the η^* and η_{boost} axes are shown in Fig 4. The final data sample is seen to lie within these regions. We also note that since we are interested only in $|\cos\theta^*|$, data appear on both sides of the η^* axis. Furthermore, we must require that all events in a particular region are above a certain p^*, which is dictated by $p^*_{min} = p_{Tmin} \cdot \cosh\eta^*_{max}$, so that all events are assured to be above the trigger threshold.

In order to extract only the $\cos\theta^*$ dependence, we normalize between regions in the areas where they overlap. Furthermore, we normalize the curve to unity in the first three bins. This allows us to compare the shape of the distribution with the next-to-leading log (NLL) theoretical prediction (1). When projecting onto the $\cos\theta^*$ axis, we always take only the data from the lower region. Thus for bins of size 0.1 in $\cos\theta^*$, the data for the first six bins ($0 \leq \cos\theta^* < 0.6$) comes from the region closest to the origin in Fig. 4, the next two bins ($0.6 \leq \cos\theta^* < 0.8$) from the middle region, and the last bin, covering $0.8 \leq \cos\theta^* \leq 0.9$, is from the outermost region.

In order to subtract the background due to jets misidentified as photons in this sample, we apply the calorimeter method, described above, to the data in region 1 only ($\cos\theta^* \leq 0.6$). This results in a photon purity of ~ 0.52. We are, at this time, unable to do the background subtraction for regions 2 or 3. Therefore we assume that the background in these regions is due to jets faking photons and has the same angular distribution as the dijet sample. We select the data sample for estimating the angular distribution of the background by taking the inclusive jet sample above 30 GeV and randomly assigning one jet the role of the photon. These events are then required to pass all cuts applied to the photon sample. Knowing the angular distribution of the background and the relative normalization of signal and background allows us to extract the signal as a function of $\cos\theta^*$. The final normalized and background-subtracted data sample is shown in Fig 5. Also shown is the NLL Monte Carlo prediction which is in excellent agreement with the background-subtracted data in the range of $\cos\theta^* \leq 0.9$.

PHOTON-JET RAPIDITY CORRELATIONS

Since the dominant direct photon production process at the Tevatron is gluon Compton scattering, an analysis of the rapidity correlation between the photon and the leading jet can provide information about the gluon distributions of the colliding hadrons. Specifically, when one fixes the angle of the photon, one can probe a range of parton momenta by looking at the angular distribution of the leading associated jet. In the following preliminary analysis the η_{jet} distributions are examined for several ranges of η_γ.

A sample of photon candidates was selected from data taken during the 1994-95 run with an integrated luminosity of 35 pb^{-1}. Standard photon identification cuts were applied. In this analysis, photons were allowed in both central ($|\eta| < 0.9$) and forward ($1.5 \leq |\eta| < 2.5$) regions of the detector. The transverse momentum of the photon was required to be greater than 45 GeV/c. Lastly, the ratio of energy in the first electromagnetic layer to the total shower energy is required to be less than 1%. This cut was applied in order to increase the photon purity of the sample. For the central rapidity region, at $E_T = 60$ GeV, this cut is estimated to increase the photon purity from 60% to 75%. Photon purity values have not yet been established for the forward η region.

In this analysis, events were binned in five different ranges of the absolute photon rapidity, η_γ. The "signed" rapidity of the jet, η_{jet}, (positive if in the same rapidity direction as

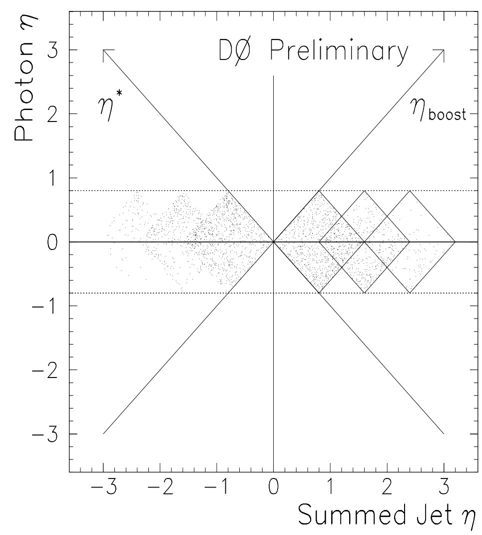

FIG. 4. Plot of candidates in η_γ vs η_{jet} for the three regions. The lines at 45° are the η_{boost} and η^* axis.

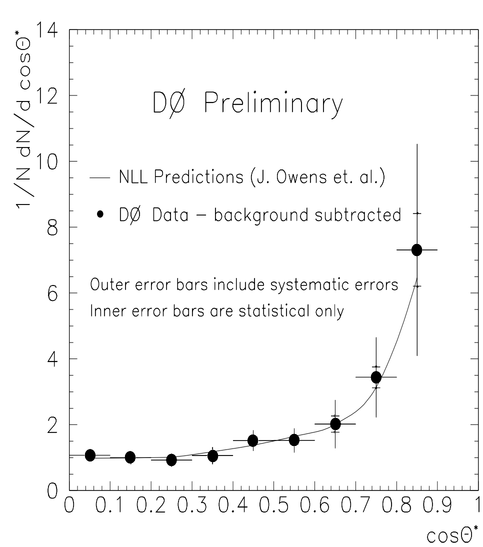

FIG. 5. Plot of the normalized $\cos\theta^*$ distribution for $gamma$ + jets events, compared to normalized NLL prediction.

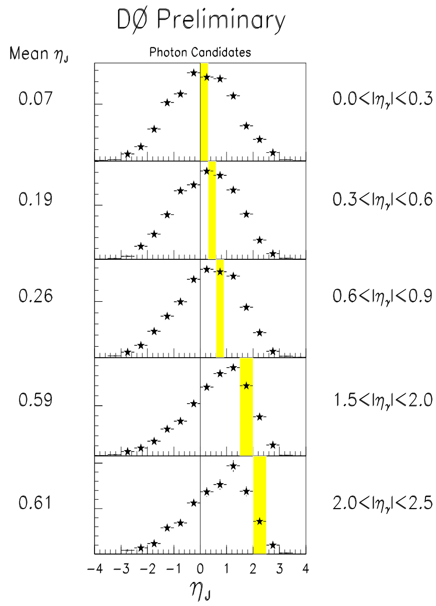

FIG. 6. η_{jet} distributions for five different regions of η_γ for the enriched photon sample. The shaded region indicates the η range covered by the photon.

the photon, negative if in the opposite) was then plotted. These distributions are shown in Fig. 6. The data show a tendency for the leading jet to follow the photon candidate forward, though not fully. The average rapidity of the leading jet is indicated for each of the η_γ regions.

As an estimate of the behavior of the background, a sample was created which was expected to discriminate *against* direct photons. Both the isolation and the longitudinal energy deposition cuts were reversed (isolation $E_T > 2$ GeV; (first EM layer)/(total shower energy)$\geq 1\%$) and one or more of other cuts expected to enhance the jet background were also required (> 2 tracks in front of the electromagnetic cluster, increased hadronic energy, non-photon-like shower shape). This background sample is expected to be dominated by jets with a large electromagnetic component. The correlation of the rapidity of the leading jet with the rapidity of this fake photon sample is shown in Fig. 7. There is a much less pronounced tendency for the leading jet to follow the electromagnetic jet (background) forward. To crosscheck the behavior of this background sample, events in this sample were compared with a sample of dijet events. The two samples gave consistent results.

Figure 8 summarizes the different behaviors of the sample expected to be enriched with photon-jet events and the sample expected to be dominated by jet-jet background. A NLL QCD prediction for photon-jet behavior (1) is also shown in Fig. 8 and, as can be seen, tends to be in qualitative agreement with the enriched photon data.

HIGH-MASS DIPHOTON PRODUCTION

A study of events containing two photons satisfying the above cuts has been carried out, both as a test of QCD processes and as a search for resonant structure in the diphoton channel.

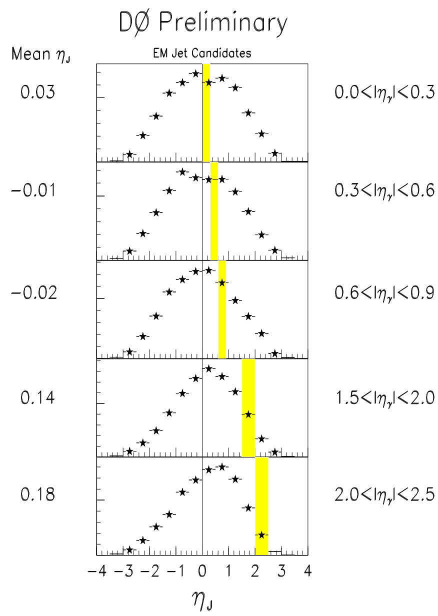

FIG. 7. η_{jet} **distributions for five different regions of "**η_γ**" for the jet-jet dominated sample. The shaded region indicates the** η **range covered by the photon.**

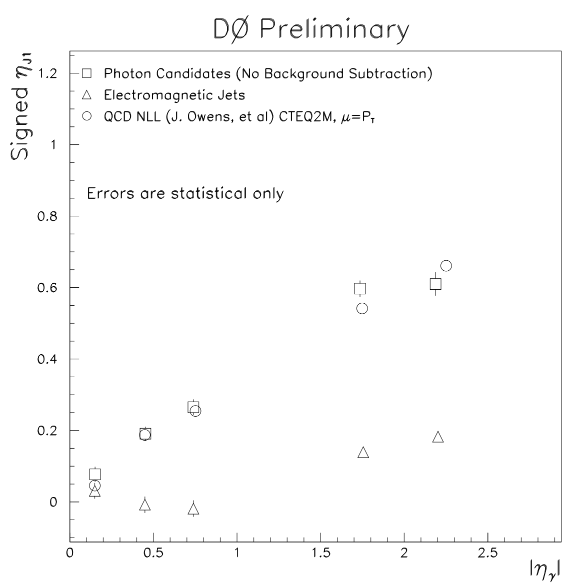

FIG. 8. **The mean of the** η_{jet} **distributions plotted as a function of the mean of each of the** η_γ **ranges.**

A particular example of resonant structure that has been suggested appears in the decay of the so-called "bosonic" Higgs. Such a particle would have standard-model strength couplings to vector bosons (including the photon), but suppressed couplings to fermions. If the fermionic decay modes are strongly suppressed, the dominant decay mode of a bosonic Higgs is into two photons (for $m_H < 90GeV$) or into $WW^{(*)}$ (for $m_H > 90GeV$).

At the Tevatron, a bosonic Higgs would be produced predominantly in association with a W or Z boson. The cross sections have been calculated (4) to be of the order of a few *pb* including the branching ratios for $W/Z \to jj$ and $H \to \gamma\gamma$, and so a few tens of events might be expected in the 1992-93 data (an integrated luminosity of 11.4 pb^{-1}). We have therefore searched for the process $(W/Z)H \to jj\gamma\gamma$ and compared with the predictions of Ref. (4).

The following cuts were imposed, chosen to be consistent with those used in the theoretical calculation of Ref. (4). Two reconstructed photons were required, with:

$$|\eta_j| < 2.5$$
$$p_{Tj} > 20GeV$$
$$\Delta R_{jj} > 0.7,\ \Delta R_{j\gamma} > 0.7$$
$$65 < m_{jj} < 105GeV$$

The two photons were required to satisfy the standard quality cuts.

This final selection yields one event with $m_{\gamma\gamma} = 60$ GeV, and none in the region above. Comparison with the theoretical prediction allows a limit to be set on the bosonic Higgs mass:

$$m_H > 73.5GeV\ (90\%\ C.L.).$$

In the 1994-1995 run, with approximately 100 pb^{-1} expected, it should be possible to extend the mass limit into the range $90 - 100$ GeV.

ACKNOWLEDGMENTS

We thank the Fermilab Accelerator, Computing, and Research Divisions, and the support staffs at the collaborating institutions for their contributions to the success of this work. We also acknowledge the support of the U.S. Department of Energy, the U.S. National Science Foundation, the Commissariat à L'Energie Atomique in France, the Ministry for Atomic Energy and the Ministry of Science and Technology Policy in Russia, CNPq in Brazil, the Departments of Atomic Energy and Science and Education in India, Colciencias in Colombia, CONACyT in Mexico, the Ministry of Education, Research Foundation and KOSEF in Korea and the A.P. Sloan Foundation.

REFERENCES

* Visitor from IHEP, Beijing, China.
‡ Visitor from CONICET, Argentina.
§ Visitor from Universidad de Buenos Aires, Argentina.
¶ Visitor from Univ. San Francisco de Quito, Ecuador.

1. B. Bailey, J.F. Owens, and J. Ohnemus, Phys. Rev. **D46:**2018 (1992).
2. S. Abachi *et al.*, (The DØ Collaboration), NIM**A338:**185 (1994).

3. J. Botts *et al.*, (The CTEQ Collaboration), Phys. Lett. **B304:**159 (1993).
4. A. Stange, W. Marciano and S. Willenbrock, FERMILAB-PUB-93/142-T.